International Journal of ChemTech Research
CODEN(USA): IJCRGG ISSN : 0974-4290
Vol.2, No.1, pp 194-204, Jan-Mar 2010

3D-QSAR and pharmacophore identification of novel imidazolyl benzimidazoles and imidazo[4,5-b]pyridines as potent p38α mitogen activated protein kinase inhibitors

Ujashkumar A. Shah, Hemantkumar S. Deokar, Shivajirao S. Kadam, Vithal M. Kulkarni*

Department of Pharmaceutical Chemistry, Poona College of Pharmacy,

Bharati Vidyapeeth University, Erandwane, Pune - 411038, India.

Corres. Author: vivivips5@gmail.com
Tel.: +91-20-24145616, Fax: +91-20-25439383

Abstract: The p38α mitogen activated protein (p38α MAP) kinase inhibitors suppress the production of proinflammatory cytokines interleukin-1beta (IL-1ß) and tumor necrosis factor-alpha (TNF-α) which are implicated in many inflammatory diseases such as rheumatoid arthritis, inflammatory bowel disease and psoriasis. Hence p38α MAP kinase inhibition has emerged as a promising therapeutic strategy for the treatment of inflammatory diseases. A series of 47 novel imidazolyl benzimidazoles and imidazo[4,5-b]pyridines derivatives has been reported as p38α MAP kinase inhibitors. A combined study of pharmacophore perception, atom based 3D-QSAR and molecular docking was undertaken to explore the structural insights of these kinase inhibitors. A five point pharmacophore (ADRRR): one hydrogen bond acceptor (A), one hydrogen bond donor (D) and three ring (RRR) features was obtained. This pharmacophore hypothesis yielded a statistically significant 3D-QSAR model with partial least-square (PLS) factor (r^2 = 0.81) for the training set of 30 compounds and PLS factors (Q^2 = 0.75, RMSE = 0.257, Pearson-R = 0.86) for the test set of 17 compounds. Docking study revealed the binding orientations of active ligand at active site amino acid residues (Met109, Lys53, Asp168 and Glu71) of p38α MAP kinase. The results of ligand based pharmacophore hypothesis and atom based 3D-QSAR give structural insights as well as highlights important binding features of novel imidazolyl benzimidazoles and imidazo[4,5-b]pyridines derivatives as p38α MAP kinase inhibitors which can provide guidance for the rational design of novel p38α MAP kinase inhibitors.
Keywords: Pharmacophore, 3D-QSAR, p38α MAP kinase, Docking.

Introduction

The p38α mitogen activated protein (p38α MAP) kinase is a serine/threonine kinase that can be activated by a range of environmental stimuli such as stress, or via the immune response. It plays an essential role in the signal transduction pathways leading to the biosynthesis of pro-inflammatory cytokines, interleukin-1ß (IL-1ß) and tumor necrosis factor-α (TNF-α) which are implicated in many inflammatory diseases.[1-3] Therefore, targeted inhibition of the p38α MAP kinase has emerged as a promising therapeutic strategy for the treatment of inflammatory diseases such as rheumatoid arthritis as well as other significant diseases where there is currently an unmet medical need such as psoriasis, Crohn's disease and inflammatory bowel disease.[4-7] Extensive efforts from many pharmaceutical companies have led to the development of several lead p38α MAP inhibitors (Figure 1) such as SB203580(SmithKline Beecham), SB-242235(GlaxoSmithKline), TAK-715(Takeda), BIRB-796(Boehringer Ingelheim), VX-745(Vertex) .[8-12]

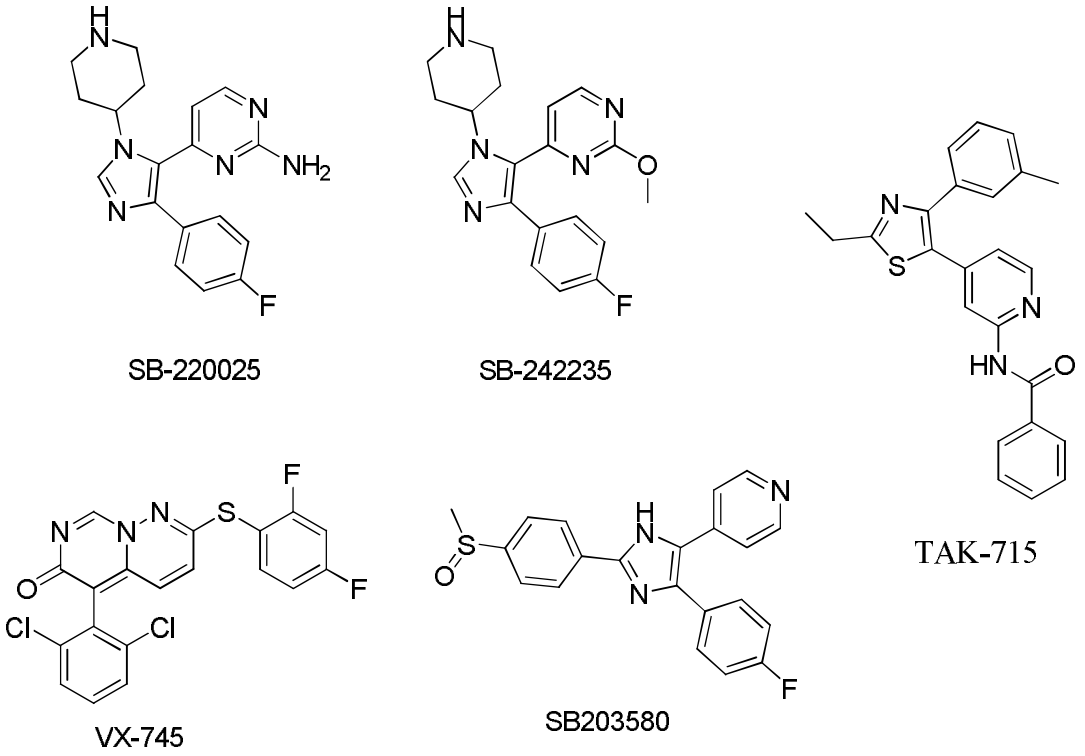

Figure 1 p38α MAP kinase inhibitors

Pharmacophore is an important and unifying concept in rational drug design that embodies the notion that molecules are active at a particular enzyme or receptor because they possess a number of chemical features that favorably interact with the target and which possess geometry complementary to it.[13] A pharmacophore hypothesis collects common features distributed in three-dimensional space representing groups in a molecule that participate in important interactions between drug and active site. In our continuing research efforts in pharmacophore development[14,15] and 3D-QSAR[16-18] of various therapeutic agents, we present here a pharmacophore perception and atom based 3D-QSAR development of a series of imidazolyl benzimidazoles and imidazo[4,5-b]pyridines as potent p38α MAP kinase inhibitors using PHASE software[19] and docking analysis by Glide software. PHASE (Pharmacophore Alignment and Scoring Engine) is a highly flexible system for common pharmacophore identification and assessment, 3D-QSAR model development and 3D database creation and searching.[20] Glide (Grid Based Ligand Docking with Energetics) has been designed to perform as close to an exhaustive search of the positional, orientation and conformational space available to the ligand as is feasible while retaining sufficient computational speed to screen large libraries. Glide uses a series of hierarchical filters to search for possible locations of the ligand in the active site region of the receptor. The objective of the present study is to develop a ligand based pharmacophore hypothesis and to derive atom based 3D-QSAR model to find features which may responsible for biological activity of imidazolyl benzimidazoles and imidazo[4,5-b]pyridines as potent p38α MAP kinase inhibitors. Further, the binding mode of the active molecule with the active site amino acid residues of p38α MAP kinase was performed by docking using Glide XP. The developed ligand based pharmacophore hypothesis gives information about important features of these derivatives for p38α MAP kinase inhibitory activity and the cubes generated from atom-based 3D-QSAR studies highlight the structural features required for p38α MAP kinase inhibition which can be useful for further design of more potent p38α inhibitors.

Experimental

Pharmacophore Modeling.

Pharmacophore modeling was carried out using PHASE running on Red Hat Linux WS 3.0. A set of 47 novel imidazolyl benzimidazoles and imidazo[4,5-b]pyridines derivatives (Table 1-4) were taken from literature for the development of ligand based pharmacophore hypothesis and atom based 3D-QSAR model.[21,22]

Table 1: *In vitro* p38α MAP kinase inhibitory activity of compounds 1-14

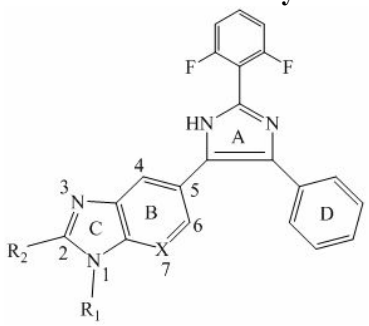

Compound	R_1	R_2	X	IC_{50} (nM)	pIC_{50} observed	pIC_{50} predicted
1*	*i*-$PrSO_2$	NH_2	CH	4.9	5.31	5.0
2*	*i*-$PrSO_2$	NHEt	CH	156	3.807	4.28
3	*i*-$PrSO_2$	N(Me)Bn	CH	2489	2.604	2.36
4	H	H	CH	88.4	4.054	3.93
5	H	NH_2	CH	131	3.883	4.01
6*	H	NHEt	CH	56.4	4.249	4.19
7*	*i*-Bu	H	CH	16.2	4.79	4.69
8	*i*-Bu	NH_2	CH	9.9	5.004	4.85
9	*i*-Bu	Me	CH	11.2	4.951	4.81
10*	CH_2-*t*-Bu	NH_2	CH	6.0	5.222	4.87
11	Ph	NH_2	CH	158	3.801	4.19
12	*i*-$PrSO_2$	NH_2	N	3.5	5.456	5.39
13	*i*-Bu	H	N	4.5	5.347	4.8
14	CH_2-*t*-Bu	NH_2	N	6.4	5.194	5.17

*Compounds used for test set.

Table 2: *In vitro* p38α MAP kinase inhibitory activity of compounds 15-26

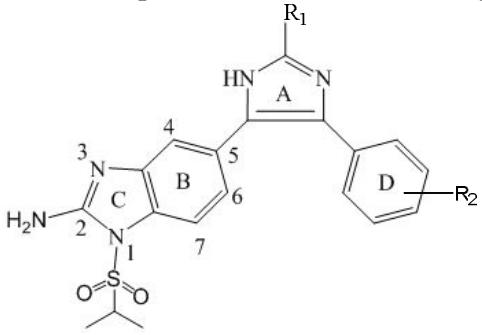

Compound	R_1	R_2	IC_{50} (nM)	pIC_{50} observed	pIC_{50} predicted
15*	*t*-Bu	2,4-F_2	4.4	5.357	5.24
16*	H	H	4.2	5.377	5.08
17	4-Pyr	H	6.1	5.215	4.95
18	4-Cl-C_6H_5	H	34.7	4.46	4.85
19	2-CF_3-C_6H_5	H	26.1	4.583	4.86
20*	2-Cl-6-F-C_6H_4	H	14.5	4.839	4.93
21	2-Cl-6-CF_3-C_6H_4	H	8.5	5.071	5.09
22	2,6-Cl_2-C_6H_4	H	15.3	4.815	5.01
23	2,6-Cl_2-C_6H_4	4-F	6.7	5.174	5.06
24*	Me	H	20.4	4.69	4.97
25*	Me	4-F	7.1	5.149	5.02
26	Me	2,4-F_2	8.8	5.056	5.12

*Compounds used for test set.

Table 3: *In vitro* p38α MAP kinase inhibitory activity of compounds 27-36

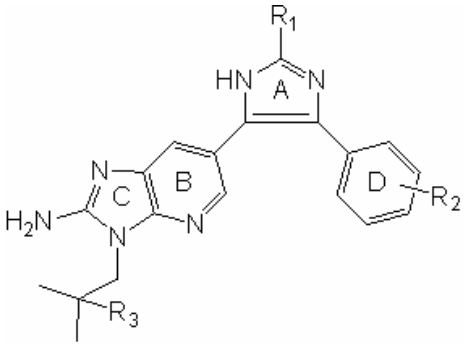

Compound	R_1	R_2	R_3	IC_{50} (nM)	pIC_{50} observed	pIC_{50} predicted
27	2,6-F_2-C_6H_4	H	H	2.5	5.602	5.29
28	2,6-Cl_2-C_6H_4	H	H	3.7	5.432	5.65
29*	*t*-Bu	H	H	5.1	5.292	5.52
30	2,6-Cl_2-C_6H_4	2,4-F_2	H	3.9	5.409	5.31
31	*t*-Bu	2,4-F_2	H	3.9	5.409	5.47
32*	2-Cl-6-F-C_6H_4	H	CH_3	3.2	5.495	5.43
33*	*t*-Bu	4-F	CH_3	7.0	5.155	5.51
34	2,6-F_2-C_6H_4	4-F	CH_3	7.2	5.143	5.3
35*	2,6-Cl_2-C_6H_4	4-F	CH_3	3.6	5.444	5.58
36*	*t*-Bu	2,4-F_2	CH_3	2.3	5.638	5.56

*Compounds used for test set.

Table 4: *In vitro* p38α MAP kinase inhibitory activity of compounds 37-47

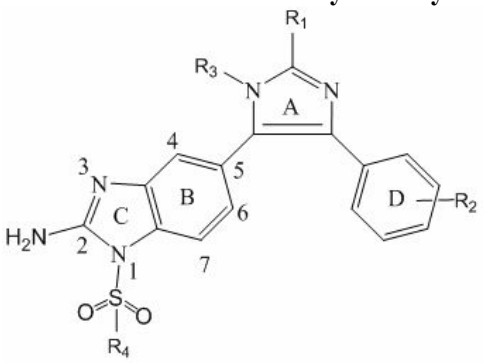

Compound	R_1	R_2	R_3	R_4	IC_{50} (nM)	pIC_{50} observed	pIC_{50} predicted
37	H	4-F	H	*i*-Pr	4.3	5.387	4.94
38	Et	4-F	H	*i*-Pr	4.7	5.328	5.08
39	*i*-Pr	4-F	H	*i*-Pr	4.5	5.347	5.09
40*	*t*-Bu	4-F	H	*i*-Pr	15.9	4.799	5.16
41	*t*-Bu	2,4-F_2	H	*t*-Bu	4.8	5.319	5.38
42	4-piperidyl	H	H	*i*-Pr	2.7	5.569	5.13
43	1-*i*-Bu-4-piperidyl	H	H	*i*-Pr	5.5	5.26	5.28
44	2,6-F_2-C_6H_4	H	H	C_5H_9	19.9	4.701	5.05
45	2,6-F_2-C_6H_4	H	H	NMe_2	22.8	4.642	4.6
46	H	4-F	Me	*i*-Pr	20.7	4.684	4.61
47*	H	4-F	4-piperidyl	*i*-Pr	125	3.903	4.41

*Compounds used for test set.

The negative logarithm of the measured IC_{50} value (pIC_{50}) of recombinant human p38α was used in the study. These 47 compounds were divided into a training set (30 compounds) and a test set (17 compounds). The training set molecules were selected in such a way that they contained information in terms of both their structural features and biological activity ranges. The most active molecules, moderately active, and less active molecules were included, to spread out the range of activities.[23] To assess the predictive power of the model, a set of 17 compounds was arbitrarily set aside as the test set.

Generation of Common Pharmacophore Hypothesis(CPH).

The common pharmacophore hypothesis (CPH) was carried out by PHASE. All molecules were built in Maestro[24] and were prepared using LigPrep with the OPLS_2005 force field.[25] Conformational space was explored through combination of Monte-Carlo Multiple Minimum (MCMM) / Low Mode (LMOD) with maximum number of conformers 1000 per structure and minimization steps 100. [26,27] Each minimized conformer was filtered through a relative energy window of 50 kJ/mol and redundancy check of 2Å in the heavy atom positions. Common pharmacophoric features were then identified from a set of variants-a set of feature types that define a possible pharmacophore-using a tree-based partitioning algorithm with maximum tree depth of four with the requirement that all actives must match. After applying default feature definitions to each ligand, common pharmacophores containing five and six sites were generated using a terminal box of 1 Å. Scoring of pharmacophore with respect to activity of ligand was conducted using default parameters for site, vector and volume terms.

Pharmacophore based QSAR do not consider ligand features beyond the pharmacophore model, such as possible steric clashes with the receptor. This requires consideration of the entire molecular structure, so an atom-based QSAR model is more useful in explaining structure activity relationship. In atom-based QSAR, a molecule is treated as a set of overlapping van der Waals spheres. Each atom (and hence each sphere) is placed into one of six categories according to a simple set of rules: hydrogens attached to polar atoms are classified as hydrogen bond donors (D); carbons, halogens, and C–H hydrogens are classified as hydrophobic/non-polar (H); atoms with an explicit negative ionic charge are classified as negative ionic (N); atoms with an explicit positive ionic charge are classified as positive ionic (P); non-ionic atoms are classified as electron-withdrawing (W); and all other types of atoms are classified as miscellaneous (X). For purposes of QSAR development, van der Waals models of the aligned training set molecules were placed in a regular grid of cubes, with each cube allotted zero or more 'bits' to account for the different types of atoms in the training set that occupy the cube. This representation gives rise to binary- valued occupation patterns that can be used as independent variables to create partial least-squares (PLS) QSAR models. Atom-based QSAR models were generated for hypotheses using the 30-member training set using a grid spacing of 1.0 Å. The best QSAR model was validated by predicting activities of the 17 test set compounds.

Docking Methodology.

Docking study was performed on Glide running on Red Hat Linux WS 3.0.[28-30] The Glide algorithm approximates a systematic search of positions, orientations and conformations of the ligand in the enzyme-binding pocket via a series of hierarchical filters. The shape and properties of the receptor are represented on a grid by several different sets of fields that provide progressively more accurate scoring of the ligand pose. The fields are computed prior to docking. The binding site is defined by a rectangular box confining the translations of the mass center of the ligand. A set of initial ligand conformations is generated through an exhaustive search of the torsional minima, and the conformers are clustered in a combinatorial fashion. Each cluster, characterized by a common conformation of the "core" and an exhaustive set of "rotamer group" conformations, is docked as a single object in the first stage. The search begins with a rough positioning and scoring phase that significantly narrows the search space and reduces the number of poses to be further considered to a few hundred. In the following stage, the selected poses are minimized on precomputed OPLS-AA van der Waals and electrostatic grids for the receptor. In the final stage, the 5-10 lowest-energy poses obtained in this fashion are subjected to a Monte Carlo procedure in which nearby torsional minima are examined, and the orientation of peripheral groups of the ligand is refined.

The crystal structure of p38α complex with SB220025 (Figure 1) was obtained from Protein Data Bank (pdb: 1BL7). All molecules were built within maestro by using build, exhaustive conformational search carried out for all molecules using OPLS_2005 force field and imposing a cutoff of allowed value of the total conformational energy compared to the lowest energy state. Minimization cycle for conjugate gradient and steepest descent minimizations used with default value 0.05 Å for initial step size and 1.00Å for maximum step size. In convergence criteria for the minimization both the energy change criteria and gradient criteria was used with default values 10-7 kcal/mol and 0.001 kcal/mol respectively. A refined enzyme structure was used for grid file generation. All amino acids within 10 Å of the SB220025 were included in the grid file generation.

Results and Discussion

Pharmacophore Generation and 3D-QSAR Model:

A total of 32 different variant hypotheses were generated upon completion of common pharmacophore identification process. Those pharmacophore models whose scores ranked in the top 1% were selected.[20] The top model was found to be associated with the five point hypotheses (Figure 2) which consist of one hydrogen bond acceptor (A), one hydrogen bond donor (D) and three ring features (RRR). This is denoted as ADRRR. The Pharmacophore hypothesis showing distance between pharmacophoric sites is depicted in figure 2.

The pharmacophore hypothesis yielded a statistically significant 3D-QSAR model with partial least-square (PLS) factors (r^2 = 0.81) for training set of 30 compounds and PLS factors (Q^2 = 0.75, root mean-squared error RMSE = 0.257, Pearson-R = 0.86) for test set of 17 compounds. The summary of atom based 3D-QSAR results is shown in Table 5. Graph of observed versus predicted biological activity of training and test set molecules are shown in figures 3 and 4 respectively.

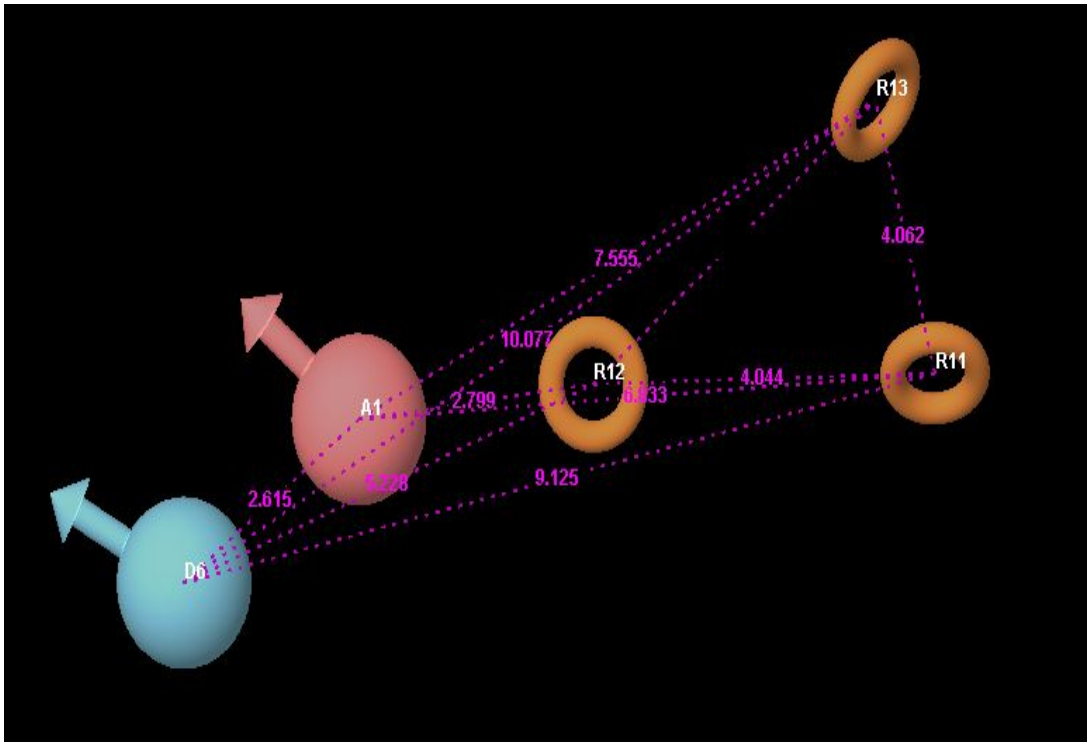

Figure 2:Pharmacophore hypothesis and distance between pharmacophoric sites. All distances are in Å unit.

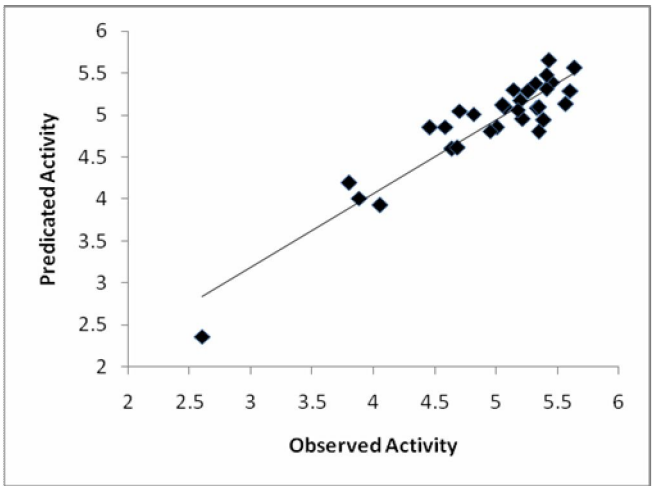

Figure. 3 Graph of observed versus predicted biological activity of training set

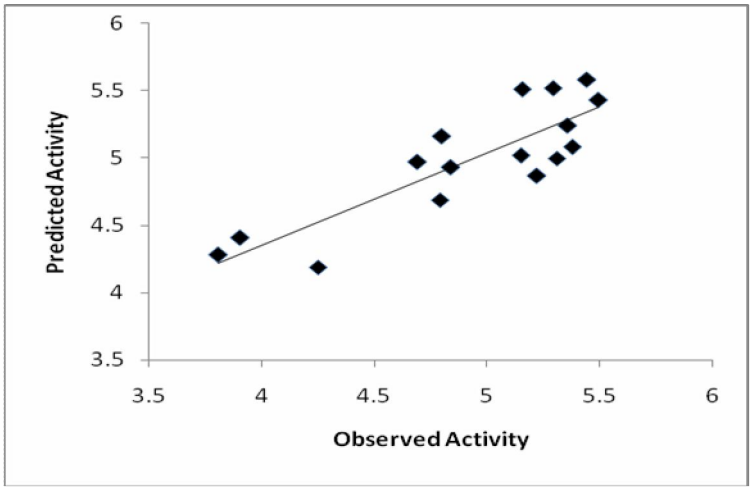

Figure 4. Graph of observed versus predicted biological activity of test set

Table 5. Summary of atom based 3D QSAR results.

Hypothesis	r^2	F	Q^2	SD	P	RMSE	Pearson-R
ADRRR	0.81	258.6	0.75	0.25	3.102e-23	0.257	0.86

SD = standard deviation of the regression, r^2 = correlation coefficient,
P = significance level of variance ratio, F = variance ratio,
Q^2 = for the predicted activities, RMSE = root-mean-square error,
Pearson-R = correlation between the predicted and observed activity for the test set

Additional insights into the inhibitory activity can be gained by visualizing the 3D-QSAR model in the context of one or more ligands in the series with diverse activity. A pictorial representation of the cubes generated for highest active and least active in the present 3D-QSAR are shown in figures 5 and 6 respectively. These generated cubes illustrate important features contributing to interactions between the ligand and the active site of an enzyme or receptor. In these representations, the blue cubes indicate favorable regions while red cubes indicate unfavorable regions for biological activity. The comparison of the most significant favorable and unfavorable interactions which arise when the 3D-QSAR model was applied to the most active reference ligand (compound 36) and the least active ligand (compound 3) which are shown in figures 5 and 6 respectively.

Figures 5 and 6 compare the most significant favorable and unfavorable hydrogen bond donor features respectively at position-2 of ring C. In figure 5, blue cubes were observed at position-2 of ring C near hydrogen bond donor vector while; red cubes were observed at position-2 of ring C near hydrogen bond donor in figure 6. This clearly indicates that presence of hydrogen bond donor at this position is better for activity. Thus, compounds having amino group at this position are more active than the compounds having mono or dialkylation at this position. These results are supported by the evidence of higher activity of compounds having amino group at this position. (compounds 10, 12, 14, 27, 35, 36, 42) and least activity of compounds having mono or dialkylation at this position (compounds 2, 3, 6, 7, 9).

More so, figures 5 and 6 compare the most significant favorable and unfavorable electron withdrawing features at position-7 of ring B. In figure 5, blue regions are observed at position-7 of ring B and red regions are observed at this position in figure 6. This suggests that presence of electronegative atom is better for activity. Therefore, introduction of electronegative atom in benzimidazole ring provided imidazopyridine ring which exhibit drastically increase in biological activity. This observation is confirmed by the fact that compounds having imidazolpyridine ring are among the highest active (compounds 12-14, 27-36) while compounds having benzimidazole ring are among the least active. (compounds 2-11).

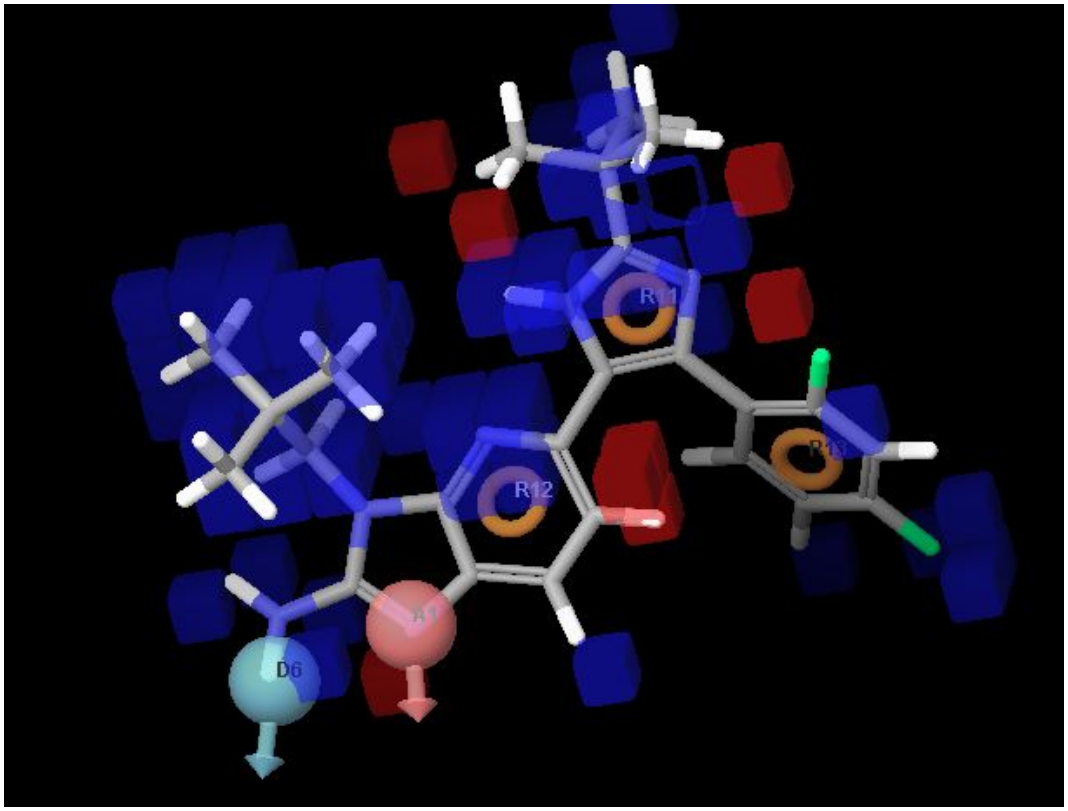

Figure 5:Atom based 3D QSAR model visualized in the context of most active compound 36. (Blue cubes indicate favorable regions while red cubes indicate unfavorable region for the activity)

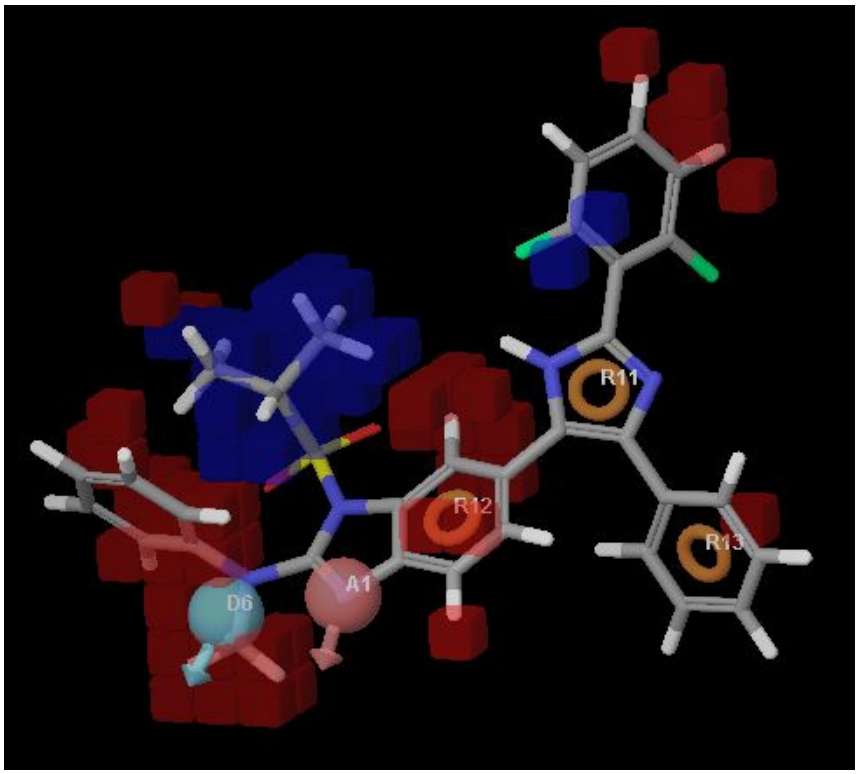

Figure 6 Atom based 3D QSAR model visualized in the context of the least active (compound 3)

Furthermore, blue cubes are observed at position-1 of ring C. This suggests that bulky substituent at this position is good for activity. This can be explained by analyzing the trends in biological data for compounds having bulky substituents at this position. Therefore, compounds having bulky substituents at this position (compounds 12-14, 27, 28, 32, 35,36) are comparatively more active than compounds having less bulky group at this position (compounds 4, 5, 6). In figure 5, blue cubes observed around ring D, this suggests that presence of electron withdrawing group on this ring is better for activity. Thus, compounds having electron withdrawing groups (compound 15, 23,35-39) at this position are comparatively more active than compounds having benzene ring at this position (compounds 1-11,17-22).

Binding mode analysis by molecular docking.

To investigate the detailed intermolecular interaction between ligand and the targeted enzyme, automated molecular docking software Glide was used to perform docking study for understanding the binding mode of the active compound 36 on p38α MAP kinase and to obtain information for further structure optimization. The docking analysis of compound 36 at p38α MAP kinase active site shows following interactions (Figure 7): The tert butyl group interacts with phosphate binding region amino acid residues (Lys53, Glu71, Asp168) and the difluorophenyl ring interacts with hydrophobic region amino acid residues (Met109, Gly110, Ala111) which play crucial role for p38α MAP kinase inhibitory activity.[31]

Conclusion

In conclusion, a highly predictive atom based 3D-QSAR model was generated using a training set of 30 molecules which consist of five point pharmacophore(ADRRR): one hydrogen bond acceptor(A), one hydrogen bond donor(D) and three ring features (RRR). The developed atom based 3D-QSAR model has provided insights into the structural requirement of novel series of imidazolyl benzimidazoles and imidazo[4,5-b]pyridines as potent p38α MAP kinase inhibitors. Atom based 3D-QSAR visualization of model in the context of the structure of molecules under study provides details of the relationship between structure and activity, and thus give information regarding structural modifications with which to design analogues with better activity prior to synthesis. . Thus, the results obtained from atom based 3D-QSAR and docking study gives a hypothetical image to design new potent p38α MAP kinase inhibitors.

The present work aimed to develop ligand based pharmacophore hypothesis and atom based 3D-QSAR give detailed structural requirement and important binding features of p38α MAP kinase which can help for the rational design of novel potent p38α MAP kinase inhibitors. Further, the results of present computational study can be used to retrieve new potential inhibitors from database using virtual screening.

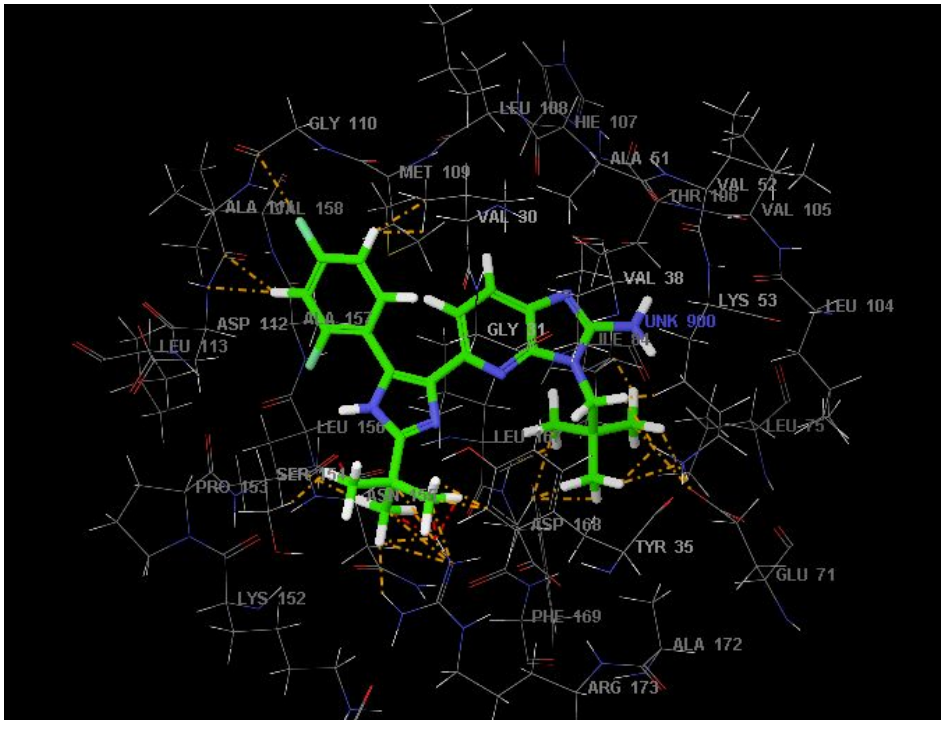

Figure 7 Docking of compound 36 in the active site of p38α MAP kinase

Acknowledgement.
The authors are thankful to Dr. K. R. Mahdik, Principal, Poona College of Pharmacy, Pune.

References

1. Lee J. C., Kassis S., Kumar S, Badger A., Adams J. L. p38 mitogen-activated protein kinase inhibitors--mechanisms and therapeutic potentials. Pharmaco. Ther., 1999, 82, 389–397
2. Adams J. L., Badger A. M., Kumar S., Lee J. C. p38 MAP kinase: molecular target for the inhibition of pro-inflammatory cytokines. Prog. Med. Chem. 2001, 38, 1-60
3. Kumar S., Boehm J., Lee J. C. p38 MAP kinases: key signalling molecules as therapeutic targets for inflammatory diseases. Nat. Rev. Drug Discovery 2003, 2, 717–726.
4. Foster M. L., Halley F., Souness J. E., Potential of p38 inhibitors in the treatment of rheumatoid arthritis. Drug News Perspect. 2000, 13, 488-497
5. Wagner G., Laufer S. Small molecular anti-cytokine agents. Med. Res. Rev. 2006, 26, 1-62
6. Hollenbach E., Neumann M., Vieth M., Roessner A., Malfertheiner P., Naumann M. Inhibition of p38 MAP kinase- and RICK/NF-kappaß-signaling suppresses inflammatory bowel disease. FASEB J. 2004, 18, 1550-1552
7. Mayer R. J., Callahan J. F. p38 MAP kinase inhibitors: A future therapy for inflammatory diseases. Drug Discov. Today Ther. Strateg. 2006, 3, 49-54
8. Badger A. M., Bradbeer J. N., Votta B., Lee J. C., Adams J. L., Griswold D. E. Pharmacological profile of SB 203580, a selective inhibitor of cytokine suppressive binding protein/p38 kinase, in animal models of arthritis, bone resorption, endotoxin shock and immune function. J. Pharmacol. Exp. Ther. 1996, 279, 1453-1461.
9. Miwatashi S., Arikawa Y., Kotani E., Miyamoto M., Naruo K., Kimura H., Tanaka T., Asahi S., Ohkawa S. Novel inhibitor of p38 MAP kinase as an anti-TNF-alpha drug: discovery of N-[4-[2-ethyl-4-(3-methylphenyl)-1,3-thiazol-5-yl]-2-pyridyl]benzamide (TAK-715) as a potent and orally active anti-rheumatoid arthritis agent. J. Med. Chem. 2005, 48, 966-5679
10. Badger A. M., Griswold D. E., Kapadia R., Blake S., Swift B. A., Hoffman S. J., Stroup G. B., Webb E., Rieman D. J., Gowen M., Boehm J. C., Adams J. L., Lee J. C. Disease-modifying activity of SB 242235, a selective inhibitor of p38 mitogen-activated protein kinase, in rat adjuvant-induced arthritis. Arthritis Rheum. 2000, 43, 175-183.
11. Regan J., Capolino A., Cirillo P. F., Gilmore T., Graham A. G., Hickey E., Kroe R. R., Madwed J., Moriak M., Nelson R., Pargellis C. A., Swinamer A., Torcellini C., Tsang M., Moss N. Structure-activity relationships of the p38alpha MAP kinase inhibitor 1-(5-tert-butyl-2-p-tolyl-2H-pyrazol-3-yl)-3-[4-(2-morpholin-4-yl-ethoxy)naph-thalen-1-l]urea (BIRB 796). J. Med. Chem. 2003, 46, 4676-4686.
12. Haddad J. J. VX-745 Vertex Pharmaceutical. Curr. Opin. Investig. Drugs 2001, 2, 1070-1076.
13. Marriott D. P., Dougall I. G., Meghani P., Liu Y. J., Flower D. R. Lead generation using pharmacophore mapping and three-dimensional database searching: application to muscarinic M(3) receptor antagonists. J. Med. Chem. 1999, 42, 3210-3216
14. Talele T. T., Kulkarni S. S., Kulkarni V. M. Development of pharmacophore alignment models as input for comparative molecular field analysis of a diverse set of azole antifungal agents. J. Chem. Inf. Comput. Sci. 1999, 39, 958-966.
15. Karki R. G., Kulkarni V. M. A feature based pharmacophore for Candida albicans MyristoylCoA: protein N-myristoyltransferase inhibitors. Eur. J. Med. Chem. 2001, 36, 147-163
16. Juvale D. C., Kulkarni V. V., Deokar H. S., Wagh N. K., Padhye S. B., Kulkarni V. M. 3D-QSAR of histone deacetylase inhibitors: hydroxamate analogues. Org. Biomol. Chem. 2006, 4, 2858-2868.
17. Gokhale V. M., Kulkarni V. M. Understanding the antifungal activity of terbinafine analogues using quantitative structure–activity relationship (QSAR) models. Bioorg. Med. Chem. 2000, 8, 2487–2499.
18. Kharkar P. S., Deodhar M. N., Kulkarni V. M. Design, synthesis, antifungal activity, and ADME prediction of functional analogues of terbinafine. Med. Chem. Res. 2009, 18, 421-432.
19. Phase, version 3.0; Schrödinger, L. L. C.: New York, USA.
20. Dixon S. L., Smondyrev A. M., Knoll E. H., Rao S. N., Shaw D. E., Friesner R. A. PHASE: a new engine for pharmacophore perception, 3D QSAR model development,

and 3D database screening: 1. Methodology and preliminary results. J. Comput. Aided Mol. Des. 2006, 20, 647–671.
21. Mader M., de Dios A., Shih C., Bonjouklian R., Li T., White W., López de Uralde B., Sánchez-Martinez C., del Prado M., Jaramillo C., de Diego E., Martín Cabrejas L. M., Dominguez C., Montero C., Shepherd T., Dally R., Toth J. E., Chatterjee A., Pleite S., Blanco-Urgoiti J., Perez L., Barberis M., Lorite M. J., Jambrina E., Nevill C. R. Jr, Lee P. A., Schultz R. C., Wolos J. A., Li L. C., Campbell R. M., Anderson B. D. Imidazolyl benzimidazoles and imidazo[4,5-b]pyridines as potent p38alpha MAP kinase inhibitors with excellent in vivo antiinflammatory properties. Bioorg. Med. Chem. Lett. 2008, 18, 179-183
22. de Dios A., Shih C., López de Uralde B., Sánchez C., del Prado M., Martín Cabrejas L. M., Pleite S., Blanco-Urgoiti J., Lorite M. J., Nevill C. R. Jr, Bonjouklian R., York J., Vieth M., Wang Y., Magnus N., Campbell R. M., Anderson B. D., McCann D. J., Giera D. D., Lee P. A., Schultz R. M., Li L. C., Johnson L. M., Wolos J. A. Design of potent and selective 2-aminobenzimidazole-based p38alpha MAP kinase inhibitors with excellent in vivo efficacy. J. Med. Chem. 2005, 48, 2270-2273
23. Golbraikh A., Shen M., Xiao Z., Xiao Y-D., Lee K-H., Tropsha A. Rational selection of training and test sets for the development of validated QSAR models. J. Comput. Aided Mol. Des. 2003, 17, 241-253
24. Maestro, version 8.5; Schrödinger, L. L. C.: New York, USA.
25. Jorgensen W. L., Maxwell D. S., Tirado-Rives J. Development and testing of the OPLS all-atom force field on conformational energetics and properties of organic liquids. J. Am. Chem. Soc. 1996, 118, 11225-11236.
26. Chang G., Guida W. C., Still W. C. An internal-coordinate Monte Carlo method for searching conformational space. J. Am. Chem. Soc. 1989, 111, 4379-4386.
27. Kolossvary I., Guida W. C. Low mode search. An efficient, automated computational method for conformational analysis: application to cyclic and acyclic alkanes and cyclic peptides. J. Am. Chem. Soc. 1996, 118, 5011-5019.
28. Glide, version 5.0; Schrödinger, L. L. C.: New York, USA.
29. Friesner R. A., Banks J. L., Murphy R. B., Halgren T. A., Klicic J. J., Mainz D. T., Repasky M. P., Knoll E. H., Shelley M., Perry J. K., Shaw D. E., Francis P, Shenkin P. S. Glide: a new approach for rapid, accurate docking and scoring. 1. Method and assessment of docking accuracy J. Med. Chem. 2004, 47, 1739-1749.
30. Halgren T. A., Murphy R. B., Friesner R. A., Beard H. S., Frye L. L., Pollard W. T., Banks J. L. Glide: a new approach for rapid, accurate docking and scoring. 2. Enrichment factors in database screening. J. Med. Chem. 2004, 47, 1750-1759
31. Wrobleski S. T., Doweykob A. M. Structural comparison of p38 inhibitor-protein complexes: A review of recent p38 inhibitors having unique binding interactions. Curr. Top. Med. Chem. 2005, 5, 1005-1016

*****